ISSN 0001-4370, Oceanology, 2007, Vol. 47, No. 6, pp. 769–787. © Pleiades Publishing, Inc., 2007.
Original Russian Text © V.G. Bondur, N.N. Filatov, Yu.V. Grebenyuk, Yu.S. Dolotov, R.E. Zdorovennov, M.P. Petrov, M.N. Tsidilina, 2007, published in Okeanologiya, 2007, Vol. 47, No. 6, pp. 827–846.

MARINE PHYSICS

# Studies of Hydrophysical Processes during Monitoring of the Anthropogenic Impact on Coastal Basins Using the Example of Mamala Bay of Oahu Island in Hawaii

**V. G. Bondur[a], N. N. Filatov[b], Yu. V. Grebenyuk[a], Yu. S. Dolotov[c], R. E. Zdorovennov[b], M. P. Petrov[b], and M. N. Tsidilina[a]**

[a] *"Aerocosmos" Scientific Center for Aerospace Monitoring, Moscow, Russia*
[b] *Institute for Water Problems of the North, Karelian Scientific Center, Russian Academy of Sciences, Petrozavodsk, Russia*
[c] *Institute for Water Problems, Russian Academy of Sciences, Moscow, Russia*
*e-mail: vgbondur@online.ru*
Received November 18, 2006

**Abstract**—This paper presents the main results of processing the data obtained in the study of hydrophysical processes during multidisciplinary monitoring of the anthropogenic impact on the coastal basin of Mamala Bay (Oahu Island, Hawaii). The results of the hydrophysical measurements carried out in August–September of 2002–2004 using stationary moorings and dropped and towed ship sensors were analyzed as the initial data. On the basis of these measurements, spatiotemporal, statistical, and spectral characteristics of different hydrophysical parameters of the marine environment in the basin of Mamala Bay were calculated, including three-dimensional components of the velocity vectors, the spectra of different components of velocities, the spectra of temperature fluctuations, and the characteristics of internal waves. The variability of the temperature fields and the correlation of the tidal phenomena with the temperature measurements and fluctuations caused by internal waves were analyzed. The materials and methods of the oceanographic studies and the results of the analysis of the meteorological and hydrological conditions are presented. The results obtained are used for a multidisciplinary analysis of the satellite and sea truth data.

**DOI:** 10.1134/S0001437007060033

## INTRODUCTION

The anthropogenic pollution of the World Ocean has a strong negative influence on the ecological systems of the ocean [9, 10]. Deep wastewater discharge is one of the most widespread sources of the anthropogenic influence on coastal basins. The influence of deep wastewater discharge leads to eutrophication of seawaters and toxic and microbiological pollution of the coastal zones of the ocean. A very high concentration of pollutants of anthropogenic origin in the surface layer of the ocean leads to a misbalance in the ecosystems and to a decrease in the bioproductivity of basins. In this relation, multidisciplinary studies of the marine environment using remote and contact measurements become extremely important.

The discharge of sewage into the sea is carried out using deep pipelines at a large distance from the coast and at significant depths to decrease the negative impacts on the coastal zones. The diffusers of sewage discharge devices are usually located below the density interface because it prevents the upwelling of sewage waters from rising to the surface. However, the density stratification of seawater is characterized by strong seasonal fluctuations. When the stratification significantly weakens, situations can appear that allow the sewage water rise up to the surface, thus, negatively influencing the ecosystems of coastal basins [3, 6]. Thus, much attention should be focused on the studies of the hydrophysical processes in the basins subjected to such anthropogenic impacts. The research of these processes is also necessary for the verification of the data obtained during the monitoring using satellite instruments [2].

The main objective of the experiments carried out in the study region of Mamala Bay in 2002–2004 was the development of the estimate and warning system for the possible pollution of the recreation zone of Oahu Island (Hawaii) [12, 16]. In 2002–2004, multidisciplinary oceanographic studies of the currents fields, turbulent mixing, internal waves, fluctuations of the ocean level, temperature, and salinity of the water, as well as wind waves, chemical-biological parameters, and hydrometeorological conditions combined with satellite observations were carried out to study the particularities of the spreading and transformation of the deep wastewater discharge. All the measurements were carried out according to unified methods over the same grid of autonomous moorings from vessels and coastal reference stations combined with remote measurements from several satellites [2, 5, 8, 12, 17].

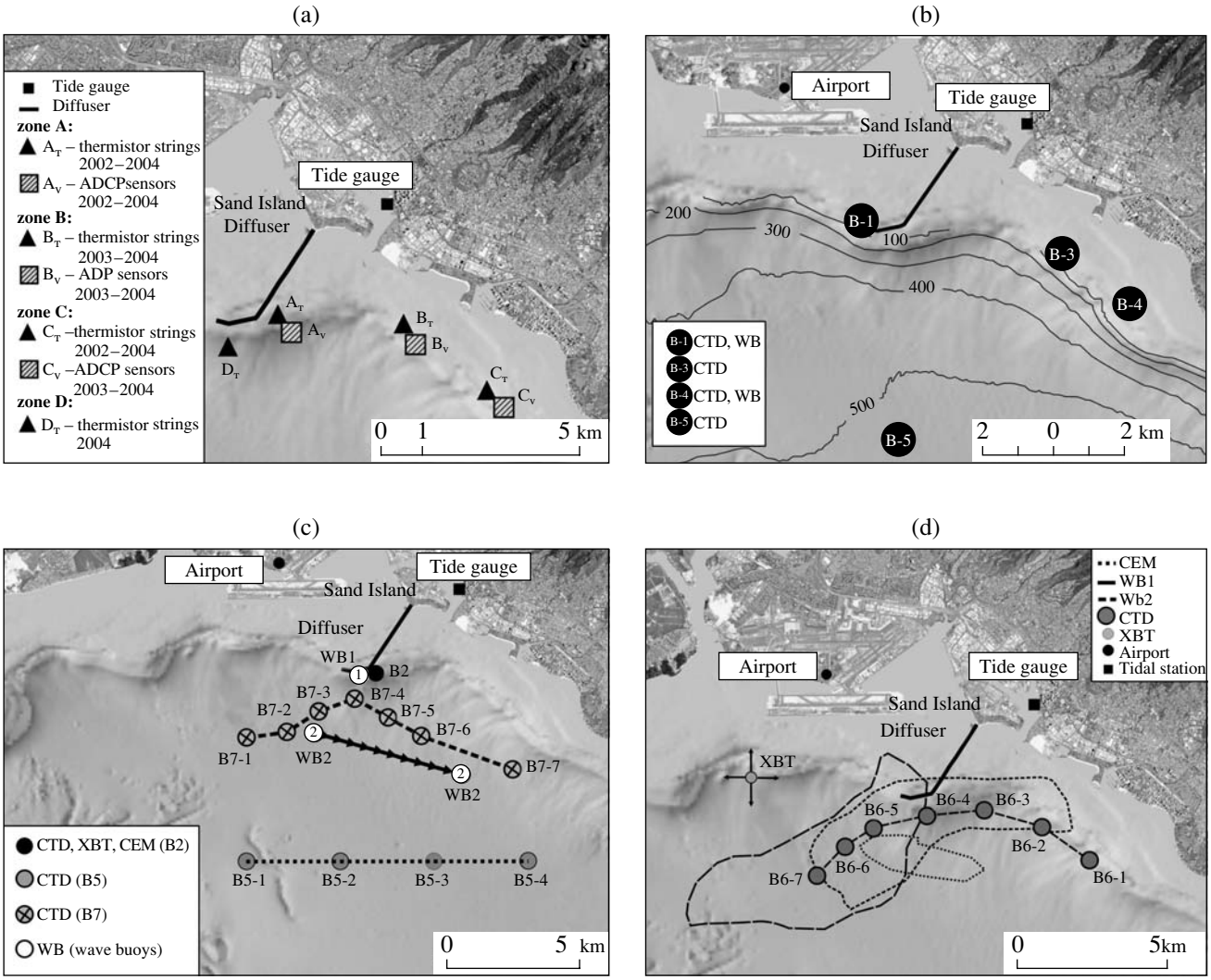


**Fig. 1.** Scheme of location of (a) moorings with ADCP, TS, Aanderaa String and measurements from ships in (b) 2002, (c) 2003, and (d) 2004.

## PARTICULAR FEATURES OF THE OBSERVATIONAL METHODS

In August–September 2002–2004, during the monitoring of the coastal region of Oahu Island (Hawaii), the hydrophysical characteristics were measured using stationary moorings as well as from a few small vessels. Both shipborne and mooring means of measurements were located in the study region to ensure the possibility of the measurements near the source of the anthropogenic impact (wastewater discharge device) and at a distance from it (2–10 km from the discharge device) at different points of the Mamala Bay basin. The temperature and vectors of the current velocity were measured using stationary mooring systems (Aanderaa, TS thermistor, ADCP profilers); drifters; and measurements from ships with CTD probes, XBTs, Compact-EM, and dropped microstructure profilers of the MSS and TOMI type [12, 13, 16].

Schemes of the location of moorings with ADCP, TS, and Aanderaa String in 2002–2004 and measurements from ships are shown in Fig. 1.

It follows from Fig. 1 that the stationary moorings were located approximately at the same points in all the years of the measurements. The places of the location of sensors can be conventionally divided into four zones: zone A near the diffuser, zone B ~3.5 km east of the diffuser, zone C ~7 km southeast of the diffuser, and zone D 1 km south of the diffuser. The difference between the schemes of the location of the sensors in different years was that, in 2004, an additional station of temperature measurements was located at point $D_T$.

Acoustic current meters ADCP (see Fig. 1a) were located at the bottom and recorded three velocity components (*Ve*, *Vn*, *Vu*) in the depth range from the bottom to 3.5 m with a 2 m interval and a sampling time of 1 min. The longest time series of the measurements was three weeks [16].

Long-term measurements of the water temperature were carried out with thermal strings (Aanderaa, TS) at moorings with sampling intervals of 5 min (Aanderaa in 2002 and 2003), 2 min (TS in 2003), and 30 s (TS in 2004) [16]. The thermal strings were located near the places of the ADCP location (see Fig. 1a).

During the field experiments, the measurements of the vertical profiles of the temperature, salinity, and density of the water were carried out from ships with CTD profilers and expendable XBT profilers (Figs. 1b–1d). In different years, 4–5 vessels were used to carry out these experiments.

Measurements with MSS (2002–2004) and TOMI (2004) microstructure profilers were also carried out from ships to obtain vertical and spatial distributions of the temperature, salinity, density, turbidity, Brunt–Väisälä frequency, and other characteristics [17, 20].

Taking into account the strong influence of tidal phenomena on different processes in the ocean basin near the Hawaii Islands during the multidisciplinary experiments, the ocean level measurements were carried out at a coastal station with a sampling interval equal to 6 min (Fig. 1).

The measurements of the wind velocity and direction were carried out using anemometers both at the Airport (2002–2004), SITTP (2003), and Kawala (2003) stationary coastal stations and from ships at different points of the basin.

An analysis of the initial data showed that the calculations were carried out with minimal sampling intervals for each process to study the high frequency fluctuations of the internal waves and currents (0.5–5 min). The minimal possible sampling interval for the cross-statistical analysis of all the hydrophysical processes was equal to 6 min (2004) and 30 min (2002 and 2003). Taking into account the sampling time and the duration of the measurements, it became possible to study the variability of the oceanographic processes on scales from a few minutes to one and a half months.

## HYDROMETEOROLOGICAL CONDITIONS DURING THE EXPERIMENTS IN MAMALA BAY IN 2002–2004

An analysis of the results of previous studies [11] showed that currents with the directions, velocities, and intensities being complex functions of the conditions (atmospheric circulation, tides, local meteorological conditions, bottom topography, and coasts, as well as seasonal variations of oceanic currents) dominate in the region. Large scale currents flowing around the island form circular flows at the lee side of the island with respect to currents. The currents over the slope of the islands are usually directed parallel to the coast generally in the western direction but can change direction to the opposite due to tides [8, 11].

During the experiments, breezes (from the island and to the island at different times of the day) and trade winds dominated. Some results of processing the characteristics of the wind regime obtained in 2004 are shown in Figs. 2a and 2b as an example. In 2002–2004, the dominating wind directions recorded at the Airport land station were located in the sector 0–80° with mean velocities of ~6 m/s and maximal velocities up to 11.5 m/s (see Fig. 2). The wind velocities recorded on the ships are within 6–8 m/s on average and tend to increase with the distance from the diffuser in the offshore direction. The maximal wind velocities reached ~11 m/s. The northeastern direction was the dominating wind direction (see Fig. 2).

The results of the cross analysis of the wind and oceanographic parameters demonstrated that the wind conditions during the sea truth experiments strongly influenced the particular features of the vertical distribution and variability of the oceanographic parameters in the upper 10-m layer.

During the field experiments, the character of the ocean level fluctuations caused by the tidal currents was approximately the same over the entire period of the observations. The maximal tide level with the dominating semidiurnal period ($M_2$ wave) was approximately 0.8 m (in 2002 and 2004) and 0.9 m (in 2003). Diurnal tidal fluctuations and multiday tidal variations were also observed (see Fig. 2c).

It is known that, in the region of the Hawaii Islands, several types of surface waves are observed [11]. First, these are wind waves generated by trade winds with heights of 1.2–3.6 m and periods of 5–8 s, which propagate to the island from the northeast almost during the entire year but reach their maximum in the summer. Second, these are storm waves opposite to the trade winds with heights of 3.0–4.5 m and periods of 8–10 s. These waves are generated by local atmospheric fronts and appear at any time of the year but prevail in the late winter or early spring. A southern swell is also recorded with heights of 0.3–1.2 m and periods of 14–22 s, which is generated by remote storms in the winter period of the Southern Hemisphere (summer and early autumn in the Hawaiian region). Finally, a northern swell is observed with heights of 2.4–4.2 m and periods of 10–15 s, which appears due to the remote storms in the north of the Pacific Ocean in the winter and early spring. However, the experiments were not carried out in that period.

An estimate of the frequency $S(\omega)$ and frequency-directional spectra in the frequency interval $0.157 \le \omega \le 3.644$ s$^{-1}$ (in the range of gravity waves) was made as a result of the analysis of the characteristics of the surface waves in the basin of Mamala Bay obtained during the experiments on wave buoys. It appeared that the one-dimensional spectra $S(\omega)$ are stable in time [2, 12]. Usually they have three quite clearly observed spectral maxima at frequencies of $\omega_{max1} \approx 0.41$ s$^{-1}$, $\omega_{max2} \approx 0.69$ s$^{-1}$, and $\omega_{max3} \approx 1.57$ s$^{-1}$. This indicates the presence of several wave systems (wind waves and swell) in the study basin.

The fields of hydrooptical characteristics were also studied using AC-9 equipment. The results of these studies are described in [2, 5].

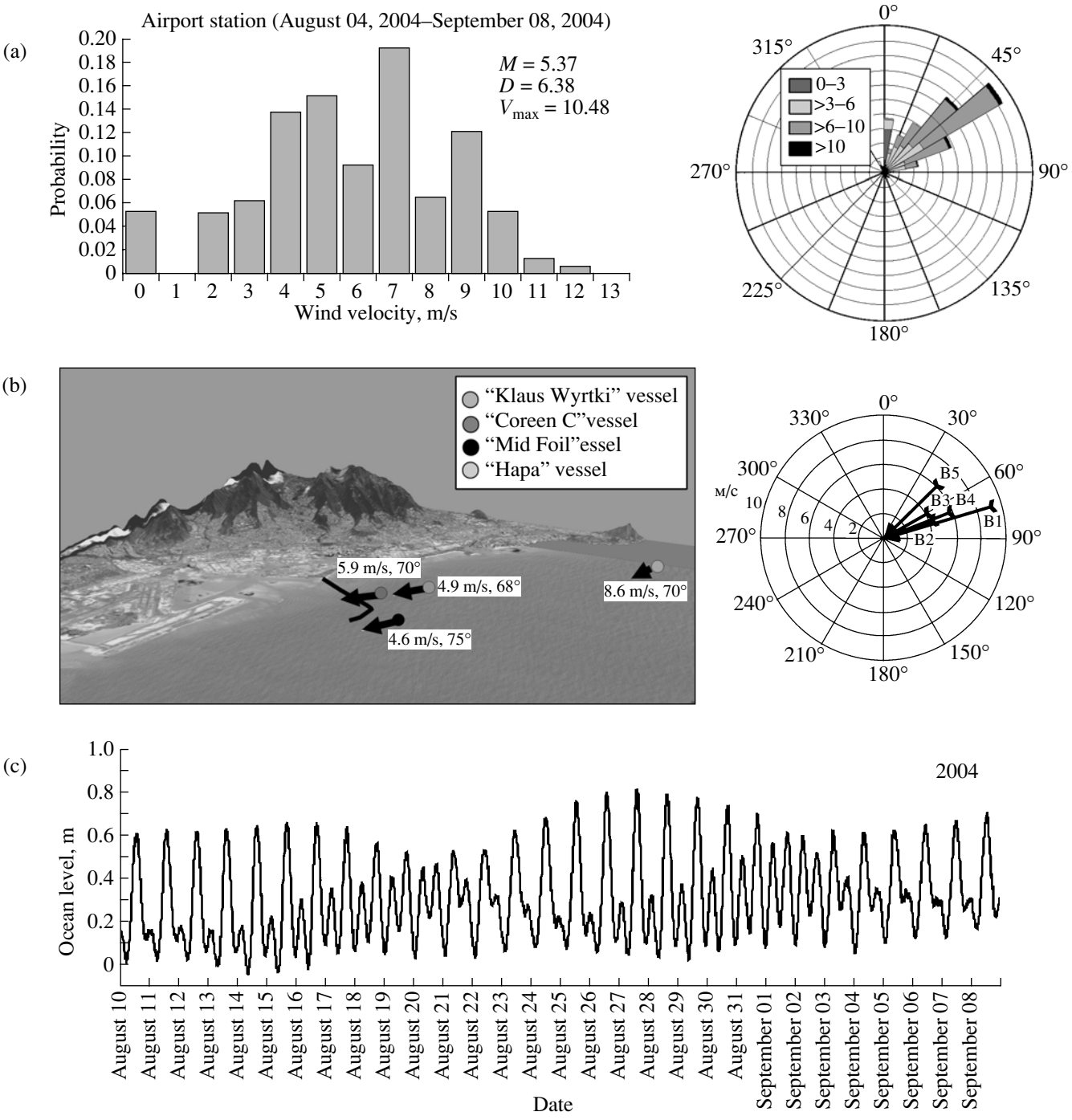


**Fig. 2.** Examples of the results of the wind data processing obtained (a) at the Airport land station in 2004 and (b) in the sea from ships on August 16, 2004. (c) Variations in the ocean level in August–September 2004.

## THE RESULTS OF THE RESEARCH OF THE CURRENT FIELDS

Long-term measurements of the current parameters in Mamala Bay were carried out using acoustic Doppler profilers ADCP [16]. As a result of the preliminary data processing, three components of the current velocities were obtained (*Ve*, *Vn*, and *Vu*) together with the absolute values of the velocities and direction of the currents at 37 levels in the depth range of 3.5–76.5 m.

Preliminary data analysis obtained using these current meters revealed strong fluctuations (with periods of a few minutes). Therefore, the initial data were smoothed and averaged to decrease the errors.

The fluctuations with 3- to 10-min periods found in the records of currents can be considered the most high-frequency components in the wide wave spectrum, which could be measured quite reliably using the equipment of the experiments. An analysis of the variability of the current field characteristics on time scales from 3 min to 1.5 days, i.e., in the frequency range from the Brunt–Väisälä N frequency to the local inertial frequency (of the order of 33 h), was carried out on the basis of the data of these experiments. It was important to determine the origin, to estimate the stability of the currents and the particular features of the generation of the fluctuations recorded, and to find the causes of the components in the spectra of the currents.

Three-dimensional and two-dimensional progressive vector diagrams at different levels were plotted to study the dominating transport direction in the study region of Mamala Bay [13]. The trajectories of the displacement of the water medium under the forcing of currents were determined as a result of plotting of these diagrams. Three-dimensional progressive vector diagrams of the currents at a depth of ~60 m plotted on the basis of the measurements in different time periods are shown in Fig. 3 as examples. The positive values in the progressive vector diagrams correspond to the northern, eastern, and upward directions, while the negative values correspond to the southern, western, and downward motions. An analysis of the diagrams showed that, in the region of the diffuser, the dominating direction of the transport was 220° (to the southwest) in all the periods and at different levels of the measurements. Strong variation in the field of the currents was observed in the region of the station located 3 km east of the diffuser. Quasi-wave fluctuations of the current field from the southwestern to southeastern directions were observed there.

The variability of the direction of the current velocity vector is strictly estimated on the basis of the probability analysis. In 2002–2004, histograms of the directions, absolute values of the current velocity vectors, and the horizontal components of the current vector at different levels were plotted on the basis of the measurements of parameters of the currents. Histograms of the recurrence of the directions of the current velocity vectors in August–September 2002 and 2004 at levels of 20 and 60 m are shown in Figs. 4a, 4b, 4e, and 4f as examples.

According to the data of the continuous measurements of the current characteristics at a station deployed near the diffuser (Fig. 1a), the distribution of the direction of the currents at the upper level had a single-mode structure (Fig. 4b) with a dominating direction of 220°–240° (in 2002) and a bimodal structure (Fig. 4a) with dominating directions of 90°–150° and 240°–320° (in 2004). In the middle layer (depths of 30–40 m) the vector of current velocity had similar directions, but the probability of the southeastern direction 100°–120° was greater. In the bottom layer, the currents feature a bimodal structure with directions of 80–120° and 240–280° with a dominating direction to the southwest, which corresponds to the main North Equatorial Current.

The measurements at the station located 3 km east of the diffuser (see Fig. 1a), showed that the southeasterly, southwesterly, and westerly currents dominated in the region (Figs. 4e, 4f).

The total transport at the station located 7 km southeast of the diffuser (at the beam of Diamond Head Mountain, see Fig. 1) was directed along the northwest–southeast line because the station was at a distance from the main alongshore current. Currents with directions about 120–130°, i.e. opposite to the main North Equatorial Current, were characterized by the greatest probability. In the middle layer (level 29.5 m) close to the level of the seasonal thermocline (levels 70 and 75 m), the direction was approximately 310°.

In the upper layers, relatively weak quasi-constant currents were observed with fluctuations caused by the local wind conditions.

At levels starting from 30 m, currents were observed with a relatively short-period variability at time scales from a few minutes to 12 h. Local wind conditions did not influence the variability of the currents at levels below 10 m. Reverse currents influenced by tides were also observed here. Sometimes, a rotation of the velocity vector was observed (during a few hours), which can be related to the tidal motions and variations in the synoptic situation as well as to tidal internal waves at the near-bottom levels (in 2003, the interface layer at the stations considered was located at the bottom). In 2002–2004, no inertial currents in a pure form were observed in the coastal study zone (with a clockwise rotation of the velocity vector) with time scales characteristic of the local latitude (i.e. close to 33 h).

An analysis of the histograms of the absolute values of current velocity showed that at the station located most closely to the diffuser and at stations located at a distance in the eastern and southeastern directions, mean values of the absolute value of current velocity in the entire water column studied were equal to 15–20 cm/s, while the maximal velocities reached 48.4–82.5 cm/s. A histogram of the absolute value of current velocity is shown in Fig. 4d, and statistical characteristics of the absolute values of current velocity for the period from September 1 to 6 in 2002–2004 are given in Table 1. These values are characteristic of the basin studied.

The variability of the horizontal components of the current velocity vector at all the levels was caused by tidal motions with a period characteristic of the semidiurnal tidal wave $M_2$, i.e. 12.4 h. When an incident tidal wave approaches the slope of Oahu Island, the velocity vector rotates with respect to the general direction (Fig. 5). Similar features of the currents were also characteristic

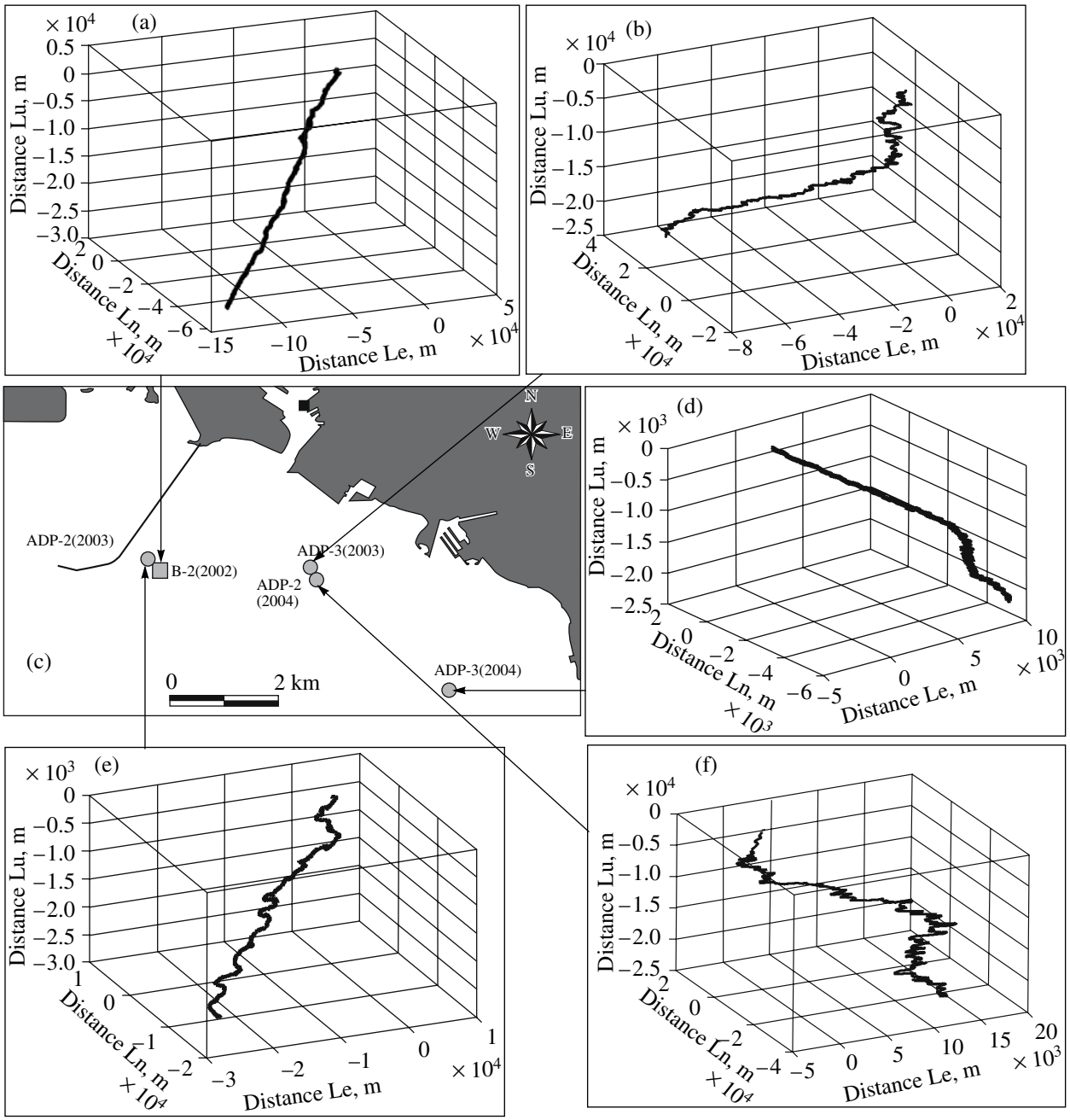


**Fig. 3.** Examples of progressive vector diagrams plotted on the basis of the measurements at a level of ~60 m in Mamala Bay in (a) 2002, (b, e) 2003, (d, f) 2004. (c) Scheme of location of the measurement points.

of station $B_V$ (see Fig. 1a) located ~3.5 km east of the diffuser.

The statistical characteristics of the currents as vector processes were estimated using the vector-algebraic method [1]. The characteristics of the tensor (invariant $I_1$ as an indicator of rotation of the currents and the variability ellipse) are shown in Fig. 6 as an example. These characteristics were obtained from the results of the measurements of currents at station $A_V$ (near the diffuser, see Fig. 1a) from September 10 to 21, 2003 (sampling interval of the measurements was 1 h; level of measurements was 31.5 m).

In 2002–2004, the tensor characteristics of the currents at the same levels (in the upper quasi-homogeneous layer, thermocline, and near-bottom layers) were approximately the same at all stations. Components with time scales of approximately 12 h close to the period of the $M_2$ tidal wave dominated in the spectrum of the currents (linear invariant) (Fig. 6a) at all the stations in the frequency range considered here. The total

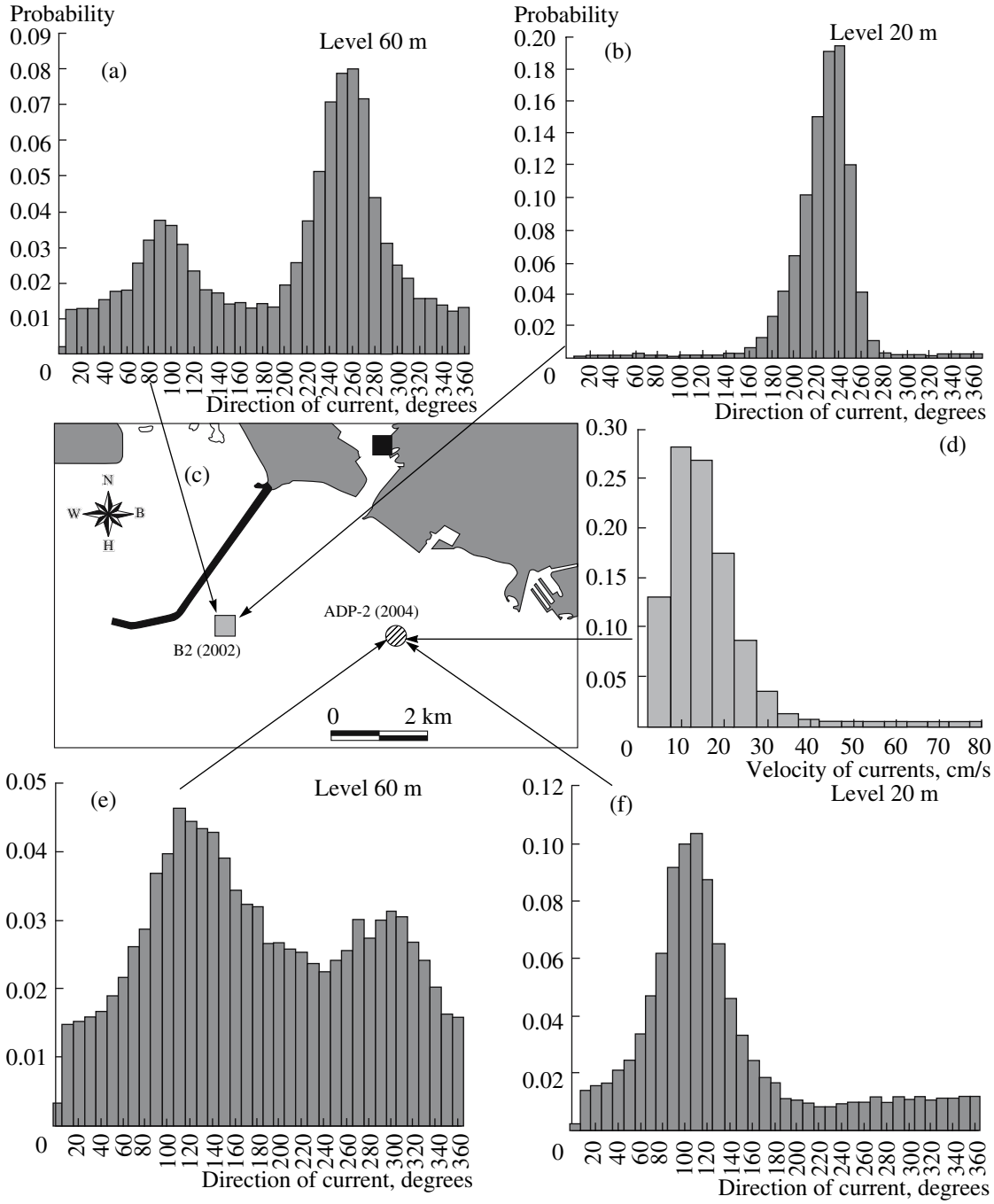


**Fig. 4.** Histograms of recurrence of directions of the currents in (a, b) September 2002, (e, f) in August–September 2004, and (d) absolute value of velocity of currents in August–September 2004. (c) Location of the experiments.

contribution of the other components to the kinetic energy was less than 15%. The features of anisotropy of the currents were estimated from the ellipses of dispersion, which showed that the large axis of the ellipse coincided with the direction of the mean flow at the given point. The ratio of the axes of the ellipses at tidal frequency varied from 0.11 to 0.13. This indicates that the water transport in the direction of the main flow dominated, which was sometimes declined by the influence of tidal motions.

An analysis of the spectra of velocity components showed that the wave and turbulent components exist in the relatively high frequency range with time scales from 1.5 h to 0.5 days [13]. Tidal motions of semidiurnal and diurnal periods dominate in the velocity spectra at all the levels (see Fig. 7).

**Table 1.** Statistical characteristics of the absolute values of the current velocities obtained from the data of the measurements using ADCP sensors from September 1 to 6, 2002–2004

| Level, m | Mean velocity, cm/s | | Variance, $cm/s^2$ | | Min velocity, cm/s | | Max velocity, cm/s | |
|---|---|---|---|---|---|---|---|---|
| | 2002 | 2003 | 2002 | 2003 | 2002 | 2003 | 2002 | 2003 |
| Near the diffuser | | | | | | | | |
| ~20 | 34.2 | 14.6 | 119.8 | 73.8 | 0.9 | 0 | 77.6 | 65.5 |
| ~30 | 25.3 | 15.49 | 133.3 | 88.79 | 0.3 | 0.1 | 67.8 | 64.2 |
| ~50 | 13.3 | 15.2 | 63.8 | 90.4 | 0 | 0 | 50.8 | 75.1 |
| ~60 | 13.4 | 15.3 | 68.0 | 95.4 | 0.1 | 0.1 | 48.4 | 65.2 |
| ~70 | – | 15.2 | – | 103.1 | – | 0 | – | 71.9 |
| ~3.5 km east of the diffuser | | | | | | | | |
| | 2003 | 2004 | 2003 | 2004 | 2003 | 2004 | 2003 | 2004 |
| ~20 | 14.9 | 20.1 | 97.3 | 114.0 | 0.1 | 0.2 | 68.5 | 59.9 |
| ~30 | 14.5 | 19.5 | 92.1 | 107.8 | 0 | 0 | 62.1 | 60.8 |
| ~50 | 14.3 | 17.4 | 86.2 | 101.6 | 0.1 | 0.1 | 62 | 67.9 |
| ~60 | 14.4 | 18.9 | 83.3 | 126.8 | 0 | 0.4 | 62.4 | 79.8 |
| ~70 | 14.3 | 19.9 | 79.0 | 135.6 | 0.1 | 0.1 | 61.7 | 82.5 |

The data obtained using drifters, which were launched during the experiments from vessels to different depths, were also used to study the features of the currents [12, 15, 17]. During the analysis, the trajectories of the drifters were compared with the directions of the dominating transports obtained on the basis of ADCP sensors at the same depths and time moments (Fig. 8). Mean values of the current velocities based on the data of drifters and ADCP sensors were also compared (Table 2). The information about the phases of tidal currents was used for a more correct analysis of the characteristics of the fields of currents.

Mean velocities of the motion of drifters at the levels of measurements (30 and 50 m) were quite close and, on the average, they were equal to 15 cm/s in 2003 and 12 cm/s in 2004. The directions of drifter motions changed in a wide range from 90° to 270°. The directions of the motion of drifters were related to the phase variations of the tidal currents.

A cross-analysis of the directions and velocities of the currents measured by the ADCP sensors and drifters showed that the current velocities measured by these instruments correlate, while the directions of currents are characterized by certain differences.

Specific peculiarities of the dependence of the depth distribution of currents on the influencing factors with account for the location of the stations of measurements were revealed on the basis of a joint analysis of the features of the tidal regime (total duration of phases of flood and ebb, velocities of increasing and decreasing of sea level) as well as the distribution of the current velocities and directions at different levels including the periods of the variations in the water mass transport in 2004 (Table 3).

In 2004, during the ebb phase an increase in the velocity of currents with depth in the upper layer was recorded during the longer duration of the phase under the conditions of a strong influence of the propagation related to the ebb currents and water transport in the southeasterly direction or in the offshore direction. During a smaller duration of the phase, a decrease in the velocity of the currents with depth was observed, which is likely to be related to a smaller influence of the ebb currents.

In the near-bottom water layer (below 70 m), only an increase in the velocity of currents with depth is observed under the same conditions at station $B_v$ (see Fig. 1a), which is related to a significant influence of the ebb currents, while at station $C_v$ (see Fig. 1a), a decrease in the velocities with depth is usually observed (it is likely, that the influence of the ebb currents here was poorer manifested).

During the flood phase, in the upper water layer, under the conditions of a relatively long phase and a significant rate of the ocean level rise associated with the water mass transport in the general southeastern direction, a decrease in the current velocities with depth was observed at station $B_v$, while at station $C_v$, their increase was found, evidently due to the greater manifestation of the tide.

In the lower layer of the water column, under the conditions of a quite long phase and a high rate of the ocean level rise, a strong difference in the distribution of the current velocities with depth was caused by the variation in the direction of the water mass transport (from southeastern to southwestern). This caused a change in the current velocities at station $B_v$ (see Fig. 1a) from an increase in the current velocities to

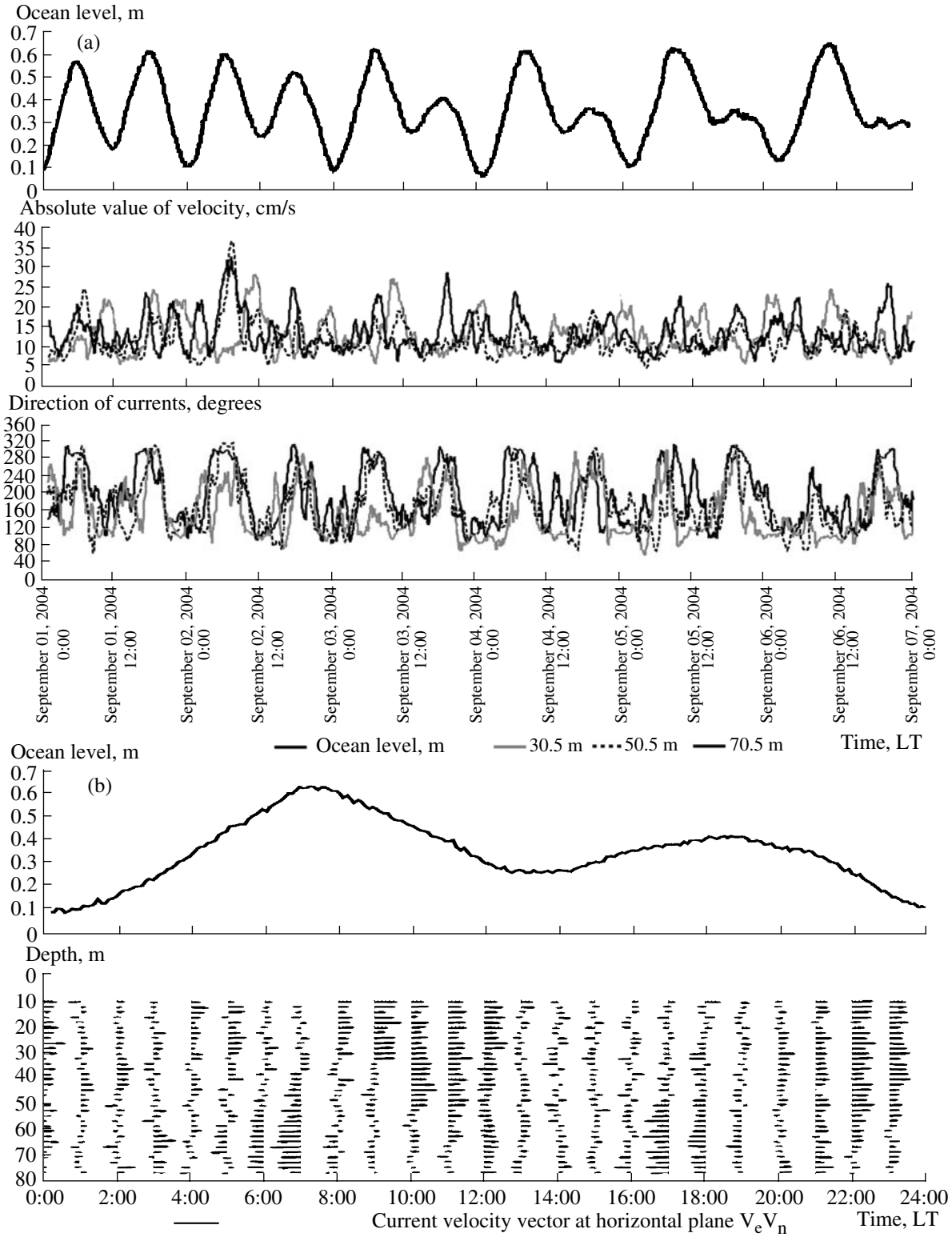


**Fig. 5.** Variability of the currents influenced by tides: (a) September 1–6, 2004; (b) September 3, 2004 (LT).

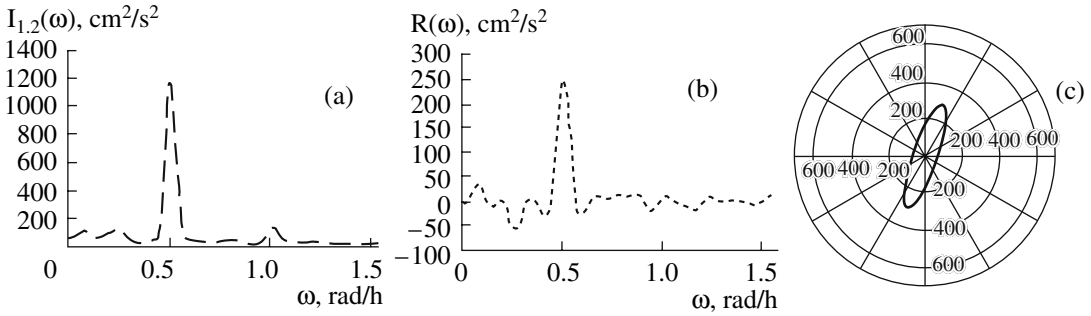


**Fig. 6.** Tensor characteristics of the currents obtained on the basis of the measurements from September 10 to September 21, 2003 at station $A_V$: (a) linear invariant of currents; (b) rotation indicator; (c) ellipse of variability. Sampling interval is 1 h, level ~30 m.

their decrease. On the contrary, at station $C_v$ (see Fig. 1a) a decrease in the velocity changed to its increase. This can be caused by the fact that the processes in the upper and lower water layers are determined by different features in their dynamical regime. At sufficiently large depths, this can be related to the general circulation around the islands including the manifestation of the North Equatorial Current.

**Table 2.** Mean values of the velocities of drifters and absolute values of current velocities measured by ADCP sensors during fixed time intervals. The directions of the motion of drifters and dominating directions of water mass transports on the basis of ADCP sensors

| Date | Level, m | | Velocity, cm/s | | Direction, degrees | |
|---|---|---|---|---|---|---|
| | ADCP | Drifter | ADCP | Drifter | ADCP | Drifter |
| September 04, 2003 | 30.5 | 30 | 16.42 | 21.70 | 257 | 270 |
| | 50.5 | 50 | 15.81 | 19.92 | 258 | 280 |
| September 06, 2003 | 30.5 | 30 | 15.69 | 9.75 | 80/85 | 122/214 |
| | 50.5 | 50 | 12.58 | 13.55 | 130/85/100 | 270/107/190 |
| September 11, 2003 | 30.5 | 30 | 17.33 | 14.19 | 214 | 180 |
| | 50.5 | 50 | 21.52 | 17.29 | 227 | 180 |
| September 13, 2003 | 30.5 | 30 | 15.34 | 14.28 | 180 | 85 |
| | 50.5 | 50 | 15.67 | 10.17 | 166/247 | 90/220 |
| September 14, 2003 | 50.5 | 50 | 10.19 | 12.85 | 180 | 120 |
| August 24, 2004 | 30.5 | 30 | 10.09 | 9.67 | 122 | 111 |
| | 50.5 | 50 | 11.56 | 8.18 | 158 | 113 |
| August 25, 2004 | 30.5 | 30 | 10.39 | 11.06 | 92 | 107 |
| | 50.5 | 50 | 14.03 | 10.67 | 136 | 112 |
| August 26, 2004 | 30.5 | 30 | 10.11 | 10.01 | 133 | 108 |
| | 50.5 | 50 | 10.93 | 7.62 | 209 | 115/230 |
| August 29, 2004 | 30.5 | 30 | 12.30 | 16.39 | 129 | 107 |
| | 50.5 | 50 | 8.83 | 12.81 | 167 | 105 |
| August 30, 2004 | 30.5 | 30 | 10.10 | 12.12 | 187 | 108 |
| | 50.5 | 50 | 10.03 | 10.14 | 139/231 | 99/346 |
| September 03, 2004 | 30.5 | 30 | 15.44 | 15.98 | 110/213 | 90/305 |
| | 50.5 | 50 | 12.23 | 13.17 | 140/194 | 90/305 |
| September 04, 2004 | 30.5 | 30 | 10.51 | 13.19 | 135 | 100 |
| | 50.5 | 50 | 12.08 | 13.18 | 153 | 103 |

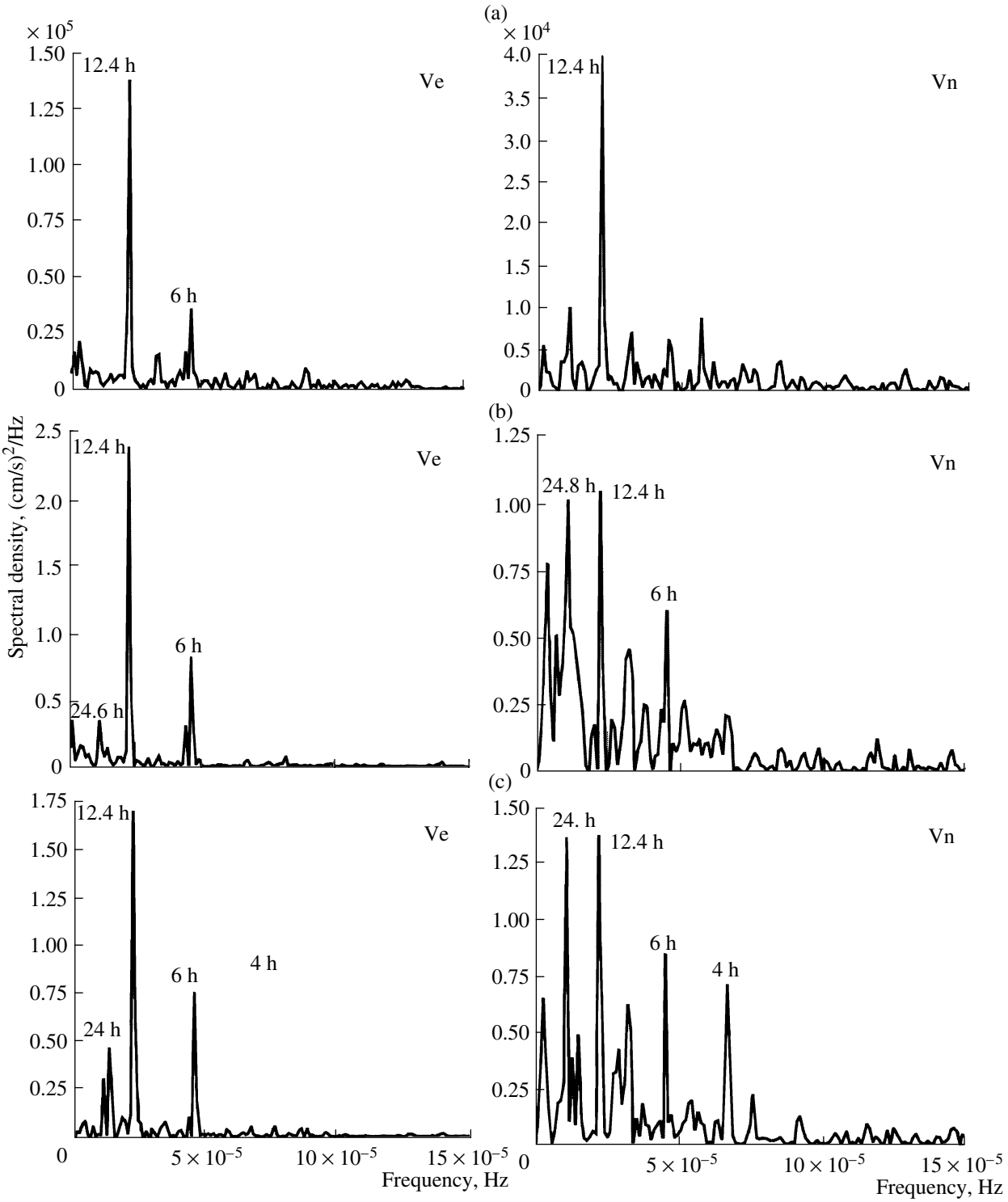


**Fig. 7.** Spectra of the horizontal components of current velocities obtained from the measurements at station $B_V$ from August 20, 2004 to September 8, 2004. Measurements at levels: (a) ~30 m, (b) ~50 m, and (c) ~70 m. Sampling interval is 1 min.

## RESULTS OF THE TEMPERATURE STUDIES

An analysis of the results of the temperature measurements in the study region showed that the thermal regime in the bay in August–September 2003 was strongly different from that observed in August–September 2002 and 2004. The charts of the vertical temperature distribution in 2003 and 2004 are shown in Fig. 9 as an example. Vertical temperature and salinity profiles at different points of the basin in 2002–2004 are shown in Fig. 10.

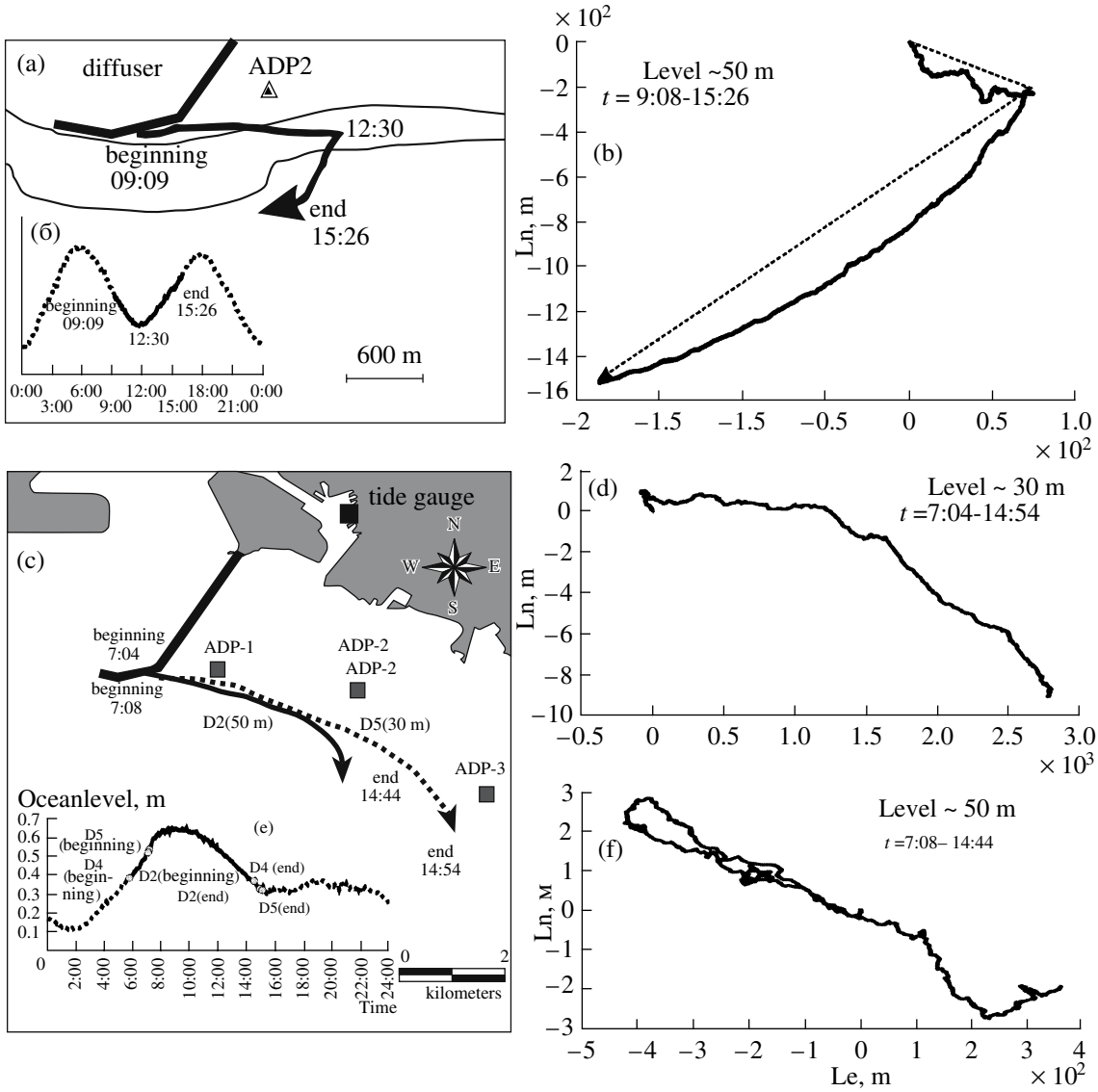


**Fig. 8.** Scheme of the motion of drifters on (a) September 13, 2003 and (d) September 5, 2004; tidal regime during the motion of drifters on (b) September 13, 2003 and (e) September 5, 2004; projections of progressive vector diagrams on the VeVn plane plotted from the ADCP sensors on (c) September 13, 2003 and (f, g) September 5, 2004.

In the temperature section in Fig. 9a in the depth–time coordinates at station $B_T$ and in the vertical profiles on the basis of CTD measurements (Figs. 10c, 10d) it is seen that, in September 2003, the well-mixed quasi-homogeneous layer with almost the same temperature values reached a depth of ~70 m. The differences in the water temperature in the surface and deep layers (50–60 m) did not exceed 0.5°C. During the major period of time, the thermocline layer was located at depths 80–100 m, while in 2002 and 2004, the thermocline was at 30–60 m. During the major period of time, mean values of the water temperature in the surface layers were equal to ~26.5°C, and at the end of September they increased to 27°C. In 2003, the variance of the temperature fluctuations at lower levels of 40–68 m exceeded the fluctuations in the upper layers of the water column. Periodical variations in the water temperature caused by tidal currents occurred in the study period at depths of 20–60 m on the basis of measurements at different stations.

In 2002 and 2004, in the basin of Mamala Bay (Oahu Island, Hawaii), a seasonal thermocline was observed, whose location varied in the range 30–60 m (see Figs. 9b, 10a, 10b, 10e, and 10g). During the field experiments in 2004, the temperature of the water column at depths of 28–70 m near the diffuser varied approximately from 22 to 28°C. The greatest temperature changes from 24 to 28°C occurred at a level close to the interface (~50 m) and at a level of ~70 m (see Fig. 9b). Statistical characteristics of the water temperature at different levels in 2004 are given in Table 4. Strong variations in the water temperature occurred during the entire period of the multidisciplinary exper-

**Table 3.** Velocities and directions of the currents and phases of tide during the experiment in 2004

| Date, Time (LT), Phase | Rate of the level change | Characteristics | Levels, m | | | | | | | |
|---|---|---|---|---|---|---|---|---|---|---|
| | | | station $B_V$ (ADSP) | | | | station $C_V$ (ADCP) | | | |
| | | | 76.5 | 70.5 | 34.5 | 28.5 | 76.5 | 70.5 | 34.5 | 28.5 |
| August 23, 2004; 10:36–19:12; ebb | 4.7 cm/h | Velocity, cm/s | 13.3 | 11.0 | 13.7 | 13.1 | 16.2 | 23.3 | 25.1 | 22.1 |
| | | Direction, deg | 141.2 | 126.4 | 106.2 | 119.6 | 132.9 | 124.9 | 117.0 | 118.3 |
| August 25, 2004; 05:42–13:00; flood | 9.2 cm/h | Velocity, cm/s | 13.7 | 11.7 | 15.2 | 15.6 | 14.6 | 18.1 | 23.2 | 22.7 |
| | | Direction, deg | 189.5 | 146.7 | 109.4 | 103.2 | 153.4 | 131.9 | 118.5 | 124.0 |
| August 29, 2004; 03:24–09:36; ebb | 5.4 cm/h | Velocity, cm/s | 12.6 | 9.8 | 11.0 | 14.1 | 16.0 | 16.5 | 15.8 | 16.6 |
| | | Direction, deg | 185.0 | 193.0 | 176.4 | 126.8 | 155.9 | 156.5 | 159.6 | 143.0 |
| August 30, 2004; 17:00–23:18; ebb | 10.2 cm/h | Velocity, cm/s | 17.9 | 11.4 | 10.9 | 15.2 | 17.7 | 18.6 | 18.0 | 24.2 |
| | | Direction, deg | 170.1 | 179.9 | 178.6 | 106.0 | 162.5 | 137.4 | 145.1 | 129.2 |
| September 03, 2004; 07:30–14:12; ebb | 5.4 cm/h | Velocity, cm/s | 13.8 | 13.0 | 13.9 | 19.1 | 24.4 | 22.1 | 23.6 | 23.8 |
| | | Direction, deg | 180.7 | 148.8 | 143.7 | 114.4 | 139.3 | 116.6 | 117.3 | 120.9 |
| September 05, 2004; 02:12–09:42; flood | 7 cm/h | Velocity, cm/s | 14.1 | 20.4 | 9.8 | 11.0 | 16.0 | 9.7 | 19.2 | 15.6 |
| | | Direction, deg | 235.6 | 215.6 | 203.1 | 140.8 | 201.2 | 180.2 | 201.4 | 148.3 |

**Table 4.** Statistical characteristics of the water temperature at stations $A_T$ and $D_T$ in 2004. Sampling interval is 1 min

| Level, m | Number of measurements | Mean, °C | Median, °C | Min, °C | Max, °C | $D$, (°C)$^2$ | σ, °C |
|---|---|---|---|---|---|---|---|
| Station $A_T$ (August 14–27, 2004) | | | | | | | |
| 33 | 18741 | 27.45 | 27.57 | 25.34 | 27.88 | 0.11 | 0.34 |
| 51 | 18741 | 26.12 | 26.30 | 23.57 | 27.79 | 1.04 | 1.02 |
| 72 | 18741 | 23.97 | 23.92 | 21.96 | 27.24 | 0.55 | 0.74 |
| Station $D_T$ (August 23– September 7, 2004) | | | | | | | |
| 28 | 21498 | 27.66 | 27.4 | 24.38 | 28.01 | 0.08 | 0.29 |
| 49 | 21498 | 26.46 | 26.56 | 23.26 | 27.82 | 0.745 | 0.86 |
| 72 | 21498 | 24.41 | 24.41 | 22.24 | 26.68 | 0.59 | 0.77 |

iment in 2004 and reached a value of $\Delta T = 3$°C at a depth of 28 m and $\Delta T = 14$°C at a depth of 170 m. As this phenomenon was observed, a fine stepwise structure with layers up to a few centimeters thick caused by mixing and internal waves were observed in the thermocline. A calculation of the Brunt–Väisälä N frequency showed that the minimal period of the fluctuations associated with internal waves in the core of the thermocline is of the order of one minute.

During the experiments in 2002 and 2004, the thermocline at a depth of 30–60 m formed a lock-layer for the sinks. The sewage discharge waters with a density smaller than that of the surrounding oceanic waters ascended to the upper layers under the buoyancy forces, reached the interface layer (lock-layer) and spread in this layer. As a result of these motions, the cloud of the discharge waters could take the so-called mushroom-shaped form, which is confirmed by the results of hydrooptical [2, 5] and microstructure [15, 17, 20] measurements. In 2003, this layer was not observed in the experiments because the thermocline was located at depths 70–100 m, i.e. below the diffuser.

The graphs of the temperature variability at different levels caused by tide in 2004 are shown in Fig. 11. It follows from this figure that strong periodical temperature time variations occurred during the study period. The main period of the variations is 12 h, which is related to the semidiurnal tide. The calculated spectra of the temperature fluctuations confirmed the strong influence of tidal currents on the variations in the temperature regime in Mamala Bay.

The temperature spectra calculated from the data of the measurements in 2004 are shown in Fig. 12. An analysis of these spectra showed that, at station $A_T$ (see

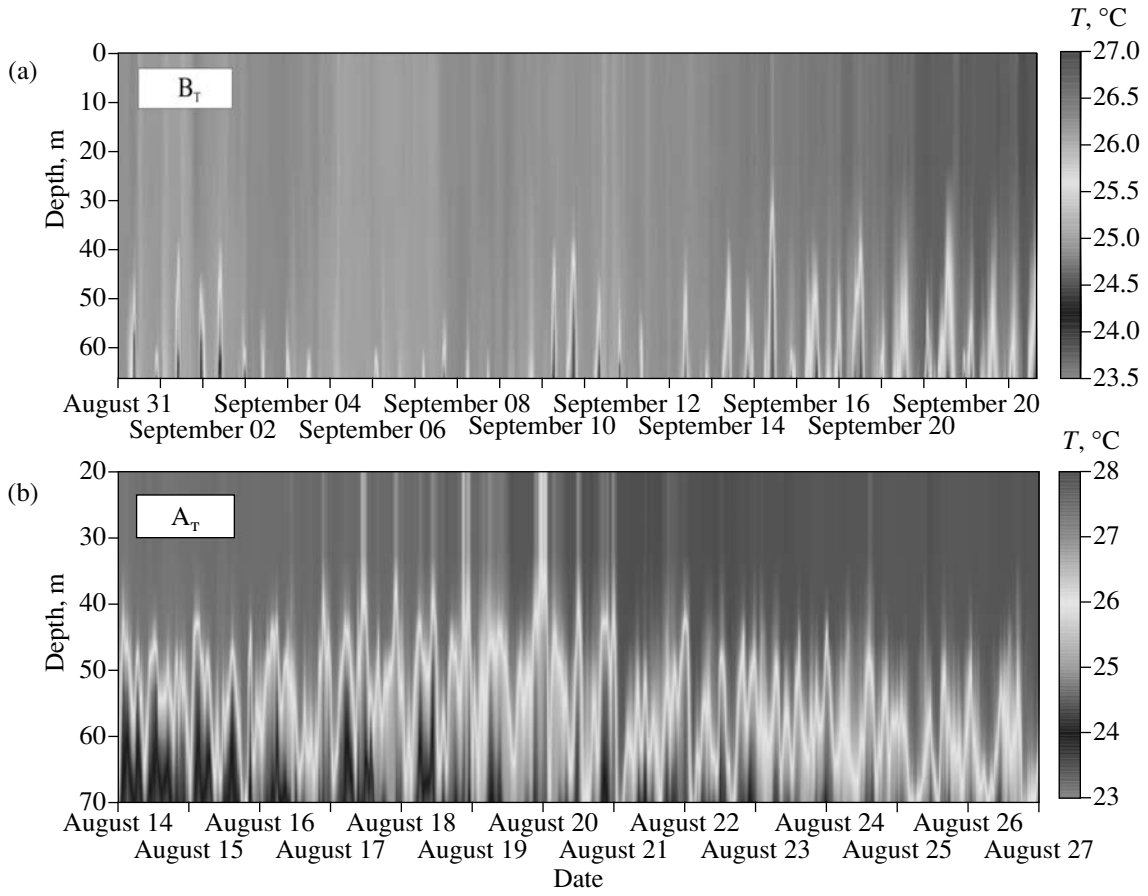


**Fig. 9.** Temperature sections with respect to the time–depth coordinate system in the layer 0–70 m obtained from the temperature string data: (a) at station $B_T$ from August 31, 2003 to September 22, 2003; (b) at station $A_T$ from August 14, 2004 to August 27, 2004.

Fig. 1a), at levels ~50 and ~70 m, the maximum of spectral energy was observed at the frequency of semidiurnal fluctuations (see Fig. 12). In the spectra obtained from the data of the measurements at other stations, the semidiurnal maximum was also manifested at other levels.

An analysis of all the temperature spectra plotted on the basis of the data during the study period showed that the main maxima of spectral energy are observed at frequencies corresponding to the periods of semidiurnal and diurnal tides and the periods of inertial oscillations (several days). Secondary maxima were also distinguished in the range of higher frequencies corresponding to periods of 4–8 h. These maxima are caused by shorter-period internal waves, which are generated during breaking of long tidal waves at the shelf break.

## RESULTS OF THE STUDY OF THE CHARACTERISTICS OF INTERNAL WAVES

A long barotropic tidal wave propagates from the open part of the basin to the continental slope [18]. Tidal currents caused by this wave propagate over the continental slope, which is an obstacle for their propagation, and obtain vertical components. Vertical components of the currents, which periodically vary, cause vertical oscillations of isopycnal surfaces. Owing to this mechanism, internal waves of tidal period are generated. As the waves propagate, they decay due to wave breaking, generation of waves of shorter periods, and turbulent viscosity [3, 4, 19].

Thus, large-scale internal waves are generated in the shelf zone under the influence of the barotropic tide, which later decay and transfer their energy to smaller size waves.

Let us consider an estimate of the internal wave fluctuations with respect to the depths of isotherms (DI) in different years. Analysis of the graphs of the 25–27°C isotherm depths in Mamala Bay (see Fig. 13) shows that the amplitude of the internal waves with time scales of semidiurnal tides reaches 40–50 m.

We note that there were not enough stations located in the form of a triangle at close distance between them to get a correct estimate of the direction of the internal wave propagation. It is possible to distinguish only the characteristics of the dominating tidal internal waves with time scales approximately equal to 24 h, 12 h, and

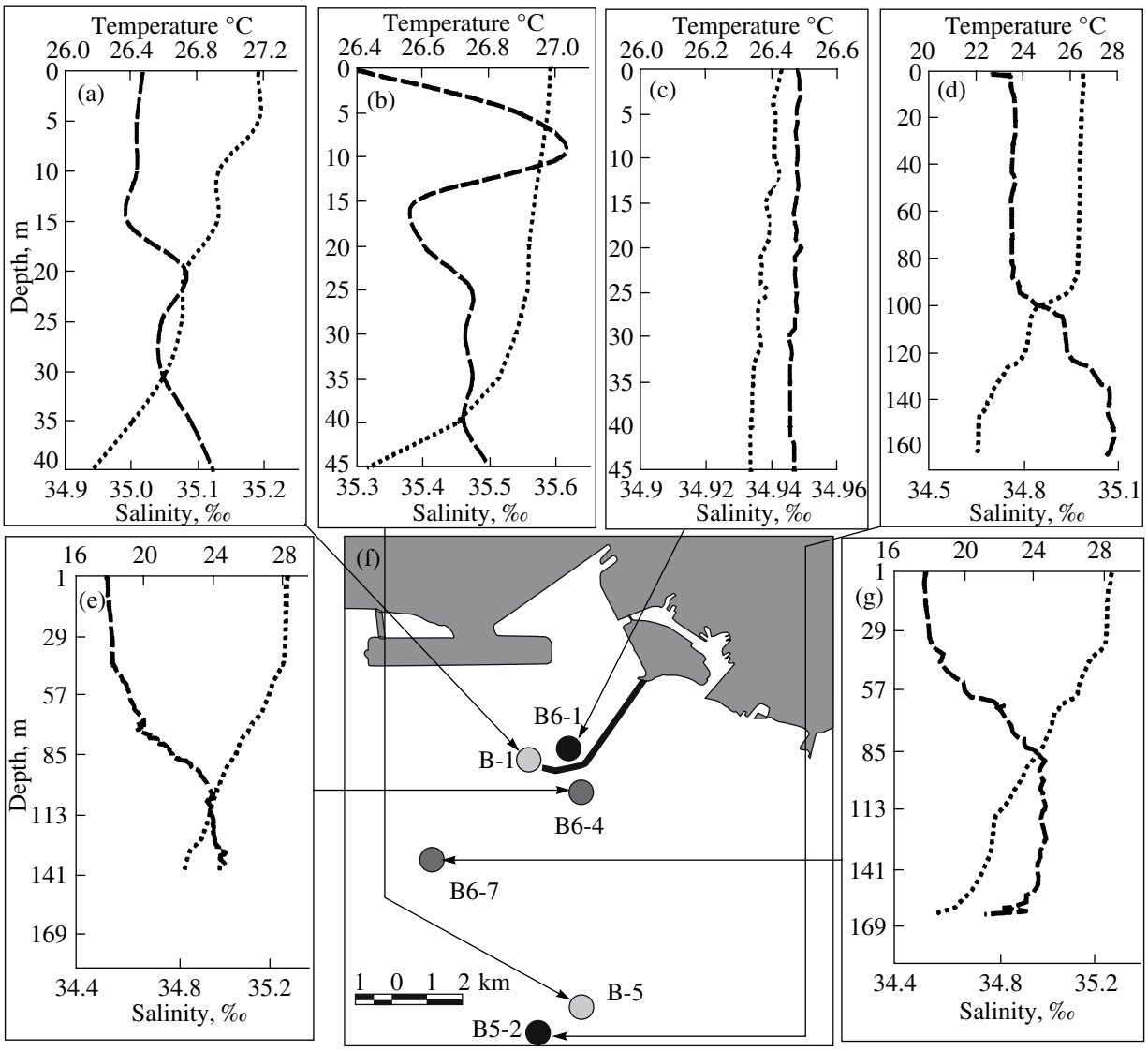


**Fig. 10.** Vertical temperature and salinity profiles plotted on the basis of the measurements: on September 02, 2002 at points (a) B-1 (b) B-5; on September 06, 2003 at points (c) B6-1 and (d) B5-2; and on September 03, 2004 at points (e) B6-4 and (g) B6-7. (f) Location of points of the measurements.

6 h, and short-period internal waves with time scales from 4 to 3 min.

In the study region we observed a statistical ensemble of internal waves with random phases and amplitudes. In the high-frequency spectral range with time scales smaller than 3 h, no significant periodical fluctuations were observed in the range studied, while the spectral slope was $\omega^{-2}$. This is typical of the spectra of internal waves in the ocean [14].

Our calculations showed that the behavior of the internal wave spectra (depths of the isotherms) is generally similar to the features of the spectra of current velocities on the scales of semidiurnal internal waves. However, the peaks at the diurnal and semidiurnal harmonics of the currents are manifested more clearly than in the spectra of isotherm depths because the variability of the currents at these frequencies was determined not only by the absolute value but also by the rotation of the vector. The lower normal mode dominates, in the case, when the thermocline is sufficiently sharply manifested (as was the case in 2002 and 2004). This can be judged from the coherence of the fluctuations at different levels. A cross-spectral analysis between three stations, at which temperature sensors were installed, allowed us to distinguish a high correlation only at the frequency corresponding to semidiurnal tides. The cross correlation of the isotherm depths at different stations is quite high (greater than 0.6), and the phase difference is close to zero. Mean heights of internal waves of the first mode (semidiurnal and tidal) were estimated from the spectra, which appeared to equal 8 m, while the maximal heights associated with this mode reach 30 m.

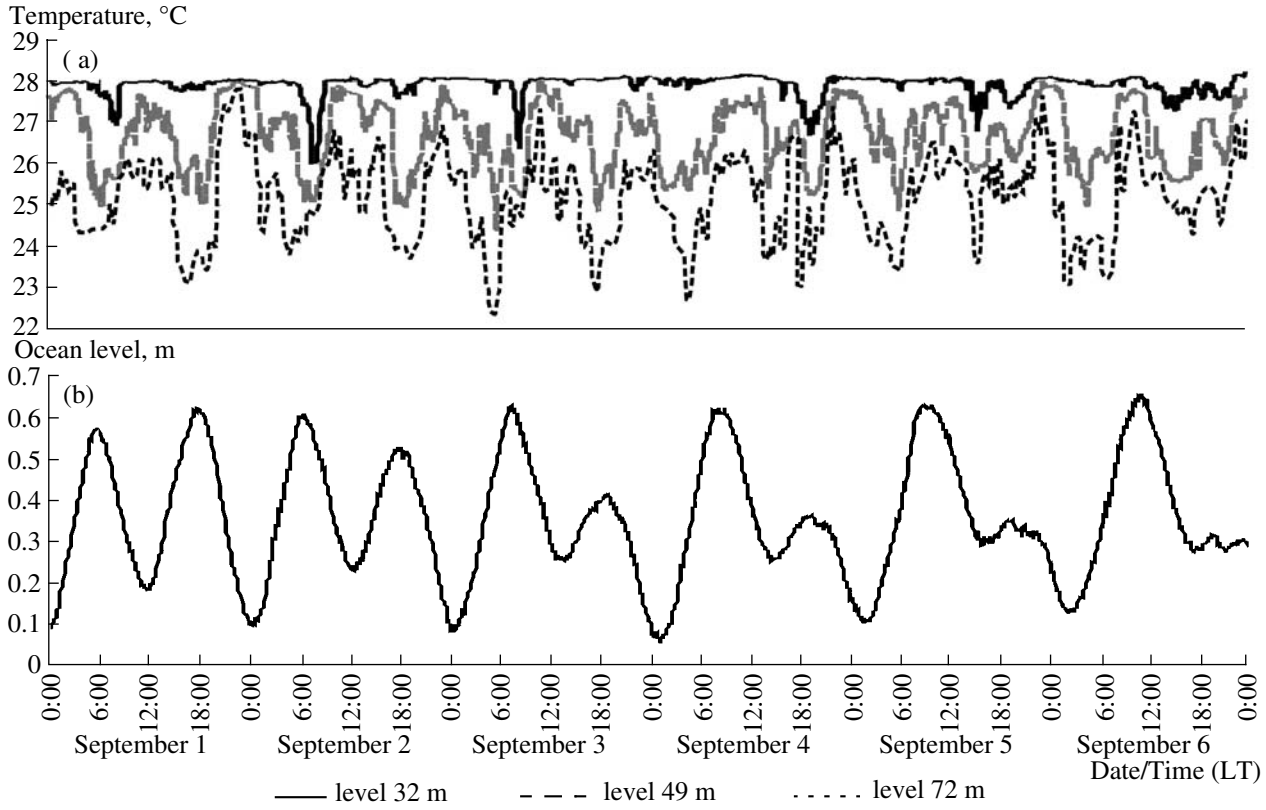


**Fig. 11.** Time variability of the temperature (a) at different levels and (b) influenced by tide during the period September 1–6, 2004.

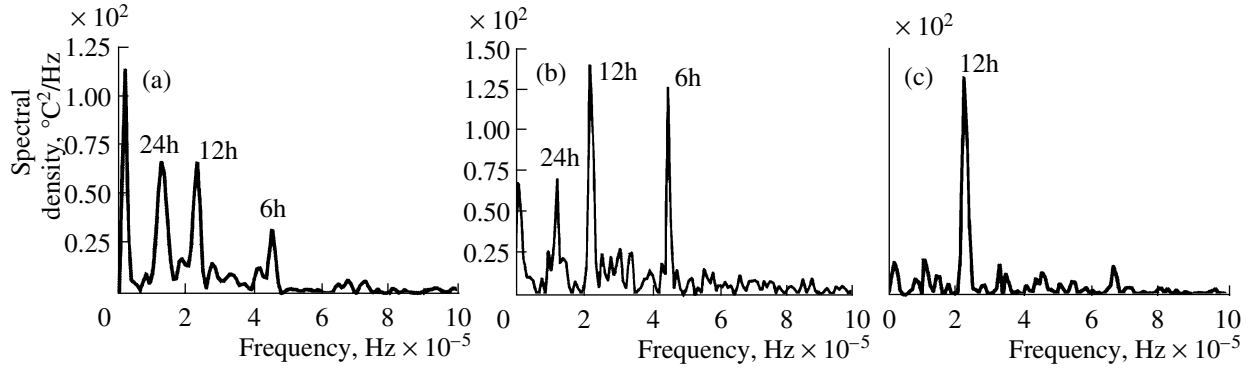


**Fig. 12.** Temperature spectra obtained from the measurements at station $A_T$ from August 14 to August 27, 2004 at levels (a) ~30 m, (b) ~50 m, and (c) ~70 m. Sampling interval of the measurements is 1 min.

Let us consider the three-dimensional frequency spectra of internal waves based on the data of fluctuations of the isotherm depths in 2002–2004 (Fig. 14). A scheme of the station location is shown in Fig. 1.

It is seen from Fig. 14 that semidiurnal and diurnal fluctuations dominate in the spectra of internal waves in the frequency range considered. It is noteworthy that the contribution of the low-frequency components of internal waves decreases with increasing energy of semidiurnal internal waves. When semidiurnal internal waves become weaker, a formation of relatively high-frequency (with periods smaller than 12 h) internal waves and harmonics of internal waves with even higher frequencies is observed. Thus, an energy transfer from one frequency range to other ranges occurs. No significant periodical fluctuations are observed in the higher frequency spectral range with time scales smaller than 3 h. Small maxima are observed in the frequency range $5 \times 10^{-3}$–$5 \times 10^{-2}$ $s^{-1}$, i.e. with periods of a few minutes.

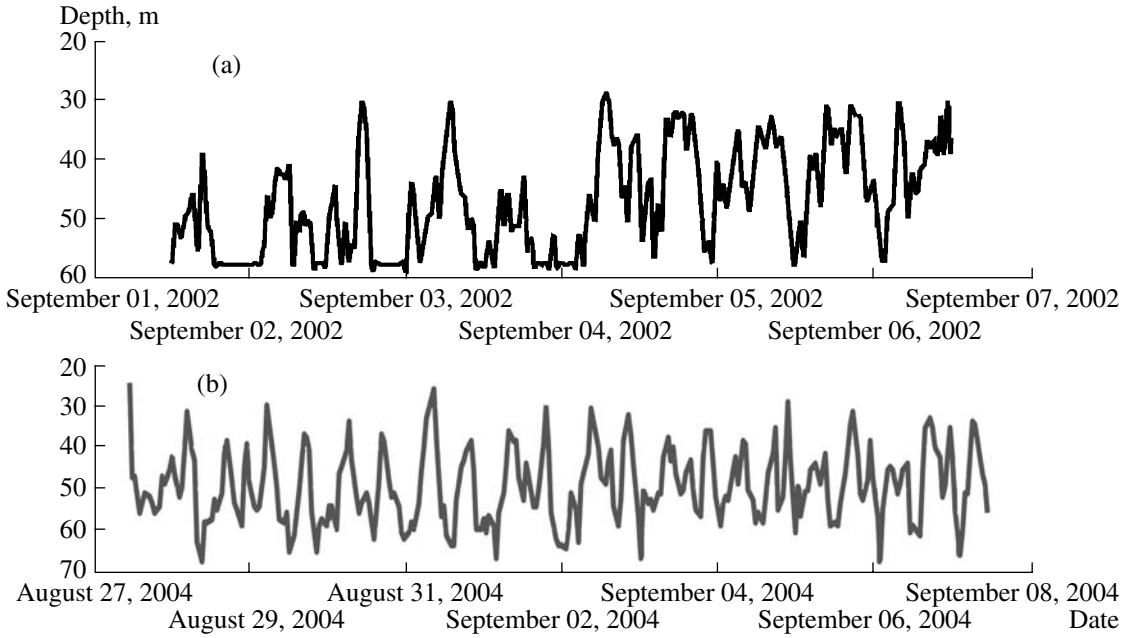


**Fig. 13.** Variations in the depth of the isotherm (a) 25°C in 2002 and (b) 27°C in 2004 at stations near the diffuser.

## CONCLUSION

It was found on the basis of an analysis of the results of processing the data obtained during the experimental studies of the hydrophysical processes in 2002–2004 in the coastal basin of Mamala Bay (Oahu Island, Hawaii) that:

(1) During the experiments, the dominating winds were of a breeze character (from the island and to the island at different times of the day) and trade winds. The dominating wind directions recorded at the land stations were in the range of 0°–80° with mean velocities of ~6 m/s and maximal velocities of 11.5 m/s. The wind velocities measured on ships were equal to 6–8 m/s on the average with a tendency to increase with the offshore distance from the diffuser. The maximal wind velocities reached ~11 m/s. The northeastern direction of the wind was dominating.

(2) A study of the characteristics of the current fields in the region of the deep wastewater discharge in Mamala Bay during the multidisciplinary field experiments showed that the dominating direction of the water transport was 220° (to the southwest) with an inclination of the general flow to the depth break. A strong variation of the current field was observed in the region of the station located 3 km to the east of the diffuser. Quasi-wave fluctuations of the direction of the current field from the southwestern to southeastern were observed against the background of the general alongshore transport.

(3) The observed variability of the horizontal components of the current velocity vector at all the depths was caused by tidal motions with a period characteristic of the semidiurnal tidal wave $M_2$. The mean absolute values of the current velocity in the entire water column were equal to 15–20 cm/s, while the maximal velocities reached 48.4–82.5 cm/s.

(4) The temperature regime during the field experiments was different in different years. In September 2003, a well-mixed quasi-homogeneous layer with close temperature values reached a depth of ~70 m. The differences in the water temperature in the surface and deep (50–60 m) layers did not exceed 0.5°C. During the major part of the time in 2003, the mean water temperatures in the surface layers were equal to ~26.5°C and, at the end of September, they reached ~27°C. In 2003, the thermocline layer was generally located at depths of 80–100 m, while, in 2002–2004, the thermocline raised to 30–60 m. During the entire period of the measurements, periodic variations in the water temperature caused by tidal currents were observed.

(5) The existence of intense internal waves of a tidal character with diurnal and semidiurnal periods was found during the analysis of the depths of the isotherms. During the experiments, internal waves of semidiurnal period had a maximal height up to 50 m, while the mean height was of the order of 8–9 m.

(6) The results obtained allow us to analyze the general outline of the hydrophysical processes in the coastal study region to estimate the degree and the character of the anthropogenic impact on the basin. These

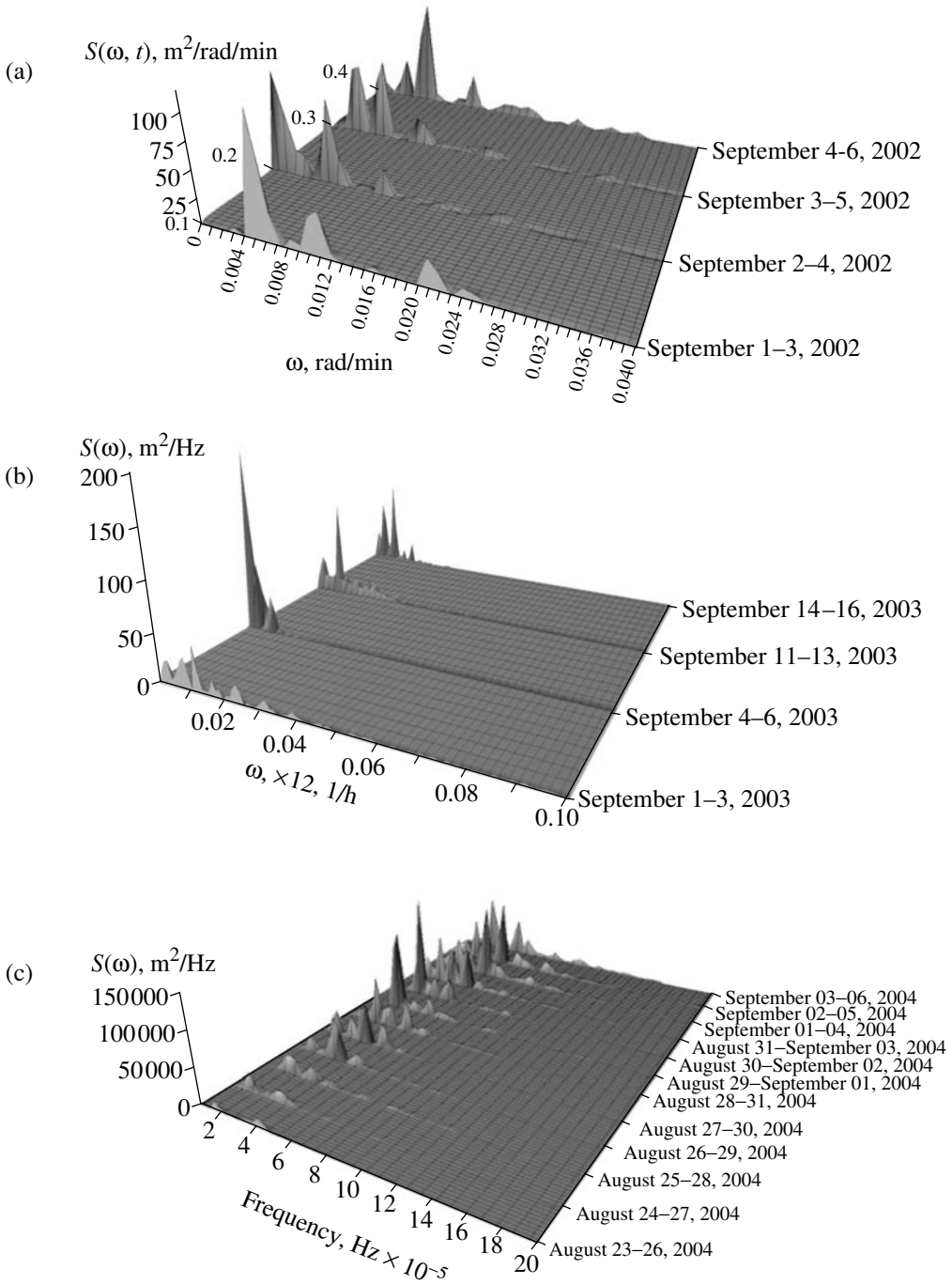


**Fig. 14.** Three-dimensional time–frequency spectra of internal waves plotted on the basis of the data of the isotherm depths: (a) 25°C at station $A_T$ in 2002; (b) 26.3°C at station $A_T$ in 2003; (c) 26°C at station $D_T$ in 2004.

results are also used in the analysis and interpretation of the results of aerospace monitoring.

## ACKNOWLEDGMENTS

The authors thank all the participants in the experiment: R.N. Keeler, C. Gibson, J. Burdette, B. Fisher, H. Prandke, F. Wolk, R. Lueck, M. Trujillo, and the crews of the vessels that took part in the experiments.

## REFERENCES

1. A. P. Belyshev, V. A. Rozhkov, and Yu. P. Klevantsov, *Probability Analysis of Sea Currents* (Gidrometizdat, Leningrad, 1983) [in Russian].
2. V. G. Bondur, *Aerospace Methods in Modern Oceanology* (New Ideas in Oceanology, Vol. 1. Physics, Chemistry, and Biology) (Nauka, Moscow, 2004) [in Russian].
3. V. G. Bondur and Yu. V. Grebenyuk, "Remote Sensing of Anthropogenic Impacts on Marine Environment Related

to Underwater Sewage Discharges: Modeling and Experiments," Issled. Zemli Kosmosa, No. 6, 59–73 (2001).

4. V. G. Bondur, E. G. Morozov, G. I. Bel'chanskii, and Yu. V. Grebenyuk, "Radiolocation Survey and Numerical Modeling of Internal Tidal Waves in the Shelf Zone," Issled. Zemli Kosmosa, No. 2, 51–63 (2006).
5. V. G. Bondur, R. N. Kiler, S. A. Starchenkov, and N. I. Rybakova, "Monitoring of Pollutions in Near-Shore Areas of the Ocean with the Use of Multispectral Satellite Images with High Spatial Resolution," Issled. Zemli Kosmosa, No. 6, 42–49 (2006).
6. V. G. Bondur, V. M. Zhurbas, and Yu. V. Grebenyuk, "Mathematical Modeling of Turbulent Jets of Deep-Water Sewage Discharge into the Coastal Bsns," Okeanologiya **46** (6), 805–820 (2006) [Oceanology **46** (6), 757–771 (2006)].
7. V. I. Vedernikov, V. G. Bondur, M. E. Vinogradov, *et al.*, "Anthropogenic Influence on the Planktonic Communities in the Basin of Mamala Bay (Oahu Island, Hawaii) Based on Field and Satellite Data," Okeanologiya **47** (2), 241–258 (2007) [Oceanology **47** (2), 221–237 (2007)].
8. *Atlas of the Oceans. The Pacific Ocean*, Ed. by S. G. Gorshkov (Glavn. Upr. Navig. Okeanogr., Moscow, 1974) [in Russian].
9. Yu. S. Dolotov, *Problems of Rational Use and protection of Coastal Areas of the World Ocean* (Nauchnyi Mir, Moscow, 1996) [in Russian].
10. Yu. A. Izrael' and A. V. Tsyban', *Anthropogenic Ecology of the Ocean* (Gidrometeoizdat, Leningrad, 1989) [in Russian].
11. *Atlas Hawaii,* Ed. by S.P. Juvik and J.O. Juvik, 3rd Edition (University of Hawaii Press, Honolulu, 1998).
12. V. Bondur, and M. Tsidilina, "Features of Formation of Remote Sensing and Sea Truth Databases for the Monitoring of Anthropogenic Impact on Ecosystems of Coastal Water Areas," in *31st International Symposium on Remote Sensing of the Environment* (ISRSE, 2006), pp. 192–195.
13. V. G. Bondur and N. N. Filatov, "Study of Physical Processes in Coastal Zone for Detecting Anthropogenic Impact by Means of Remote Sensing," in *Proceedings of the 7th Workshop on Physical Processes in Natural Waters, July 2–5, 2003* (Petrozavodsk, 2003), pp. 98–103.
14. C. J. R. Garrett and W. H. Munk, "Internal Waves at the Ocean," Annual Review of Fluid Mechanics **11**, 339–369 (1979).
15. C. H. Gibson, V. G. Bondur, R. N. Kuler, P. T. Leung, "Energetics of the Beamed Zombie Turbulence Maser Action Mechanisms for Remote Detection of Submerged Oceanic Turbulence" // J. of Applied Fluid Mechanics. **1** (1), 11–42 (2006).
16. R. N. Keeler, V. G. Bondur, and D. Vithanage, "Sea Truth Measurements for Remote Sensing of Littoral Water," Sea Tech. **45**, 53–58 (2004).
17. R. N. Keeler, V. G. Bondur, and K. H. Gibson, "Optical Satellite Imagery Detection of Internal Wave Effects from a Submerged Turbulent Outfall in the Stratified Ocean," Geoph. Res. Lett. **32**, L12610.
18. M. A. Mernifield, M. L. Eich, and M. H. Alford, "Structure and Variability of Semidiurnal Internal Tides in Mamala Bay, Hawaii," Geoph. Res **109**, C05010 (2004).
19. A. A. Petrenko, B. H. Jones, T. E. Dickey, and P. Hamilton, "Internal Tide Effects on a Sewage Plume at Sand Island, Hawaii," Conf. Shelf, **20**, 1–13 (2000).
20. F. Wolk, H. Prandke, and C. G. Gibson, "Turbulence Measurements Support Satellite Observations," Sea Tech. **45**, 47–52 (2004).